Strangeness in the nuclear medium – from hypernuclei to kaonic nuclei.

J. Mareš
Nuclear Physics Institute, 250 68 Řež, Czech Republic

Abstract
Many-body systems with nonzero strangeness are investigated within the relativistic mean field approach. Present discussion covers the spin-orbit splitting in Λ hypernuclei, the analysis of Σ^--atom data by using a Σ-nucleus optical potential, and dynamical calculations of $\bar{K}$-(hyper)nuclei.

1 Introduction

This contribution reviews our study of hyperon-nucleus and K^--nucleus interactions within the relativistic mean field (RMF) theory. This approach has been extremely successful in nuclear structure as well as nuclear dynamics calculations [1]. Attempts for its extrapolation to more general many-body hadronic systems with strangeness are thus justified.

Hypernuclei, as bound objects of different types of baryons, represent a sound generalization of traditional nuclear matter to a many-body baryonic system. Their study provides a direct test of various models for the baryon-baryon and baryon-nucleus interactions. There is a fair amount of data on Λ hypernuclei, including production, structure and decay (current status of strange particle physics is reviewed in Ref. [2]). Much less is known about strangeness $S = -2$ (Ξ or $\Lambda\Lambda$) systems or even about kaonic nuclei. Unfortunately, the missing information is crucial for extrapolating to strange matter, which is of much interest in astrophysics [3] and in the physics of heavy ion collisions [4].

RMF calculations [5] taking into account the Lorentz-tensor coupling of the ω meson to the Λ hyperon have proved that a consistent description of both nuclear and hypernuclear systems can be achieved. This is regarded a great success of the Dirac approach. Once the RMF model accounted for the hypernuclear data it was rather straightforward to extend considerations to more "strange" objects – multiply strange baryonic systems [6–8].

Calculations of Σ^- atoms not only revealed that the RMF model is capable of high quality fits to the data but also demonstrated that the data are sufficient to constrain the couplings of mesons to a Σ hyperon [9]. This has important consequences for the spectroscopy of Σ hypernuclei.

The $\bar{K}$-nucleus interaction near threshold is strongly attractive and absorptive as derived from the strong interaction shifts and widths in kaonic-atom levels [10]. The calculations existing to date for the $\bar{K}$-nucleus interaction give essentially two different predictions. Global density dependent fits to K^--atom data [11] lead to optical potentials $150 - 200$ MeV deep, whereas coupled-channel calculations based on chirally inspired models of the $\bar{K}N$ interaction [12] yield relatively shallow potentials with depth $\approx 50 - 60$ MeV. The depth of the $\bar{K}$-nucleus potential is closely related to the existence of $\bar{K}$-nuclear states and their anticipated widths. This issue has received considerable attention recently (for an overview of $\bar{K}N$ and $\bar{K}$-nucleus dynamics, see Ref. [13]).

We explored dynamical aspects of the $\bar{K}$ - nucleus interaction, with the main objective to place lower limits on the widths of possibly deeply bound $\bar{K}$-nuclear states [14]. Moreover, we studied whether the binding energy per $\bar{K}$ meson in multi-$\bar{K}$ systems increases sufficiently upon adding a large number of $\bar{K}$ mesons, so that $\bar{K}$ mesons provide the physical degrees of freedom for self-bound strange hadronic systems [15]. Kaon condensation in nuclear matter would occur beyond some threshold value of strangeness, if the binding energy per $\bar{K}$ meson exceeds the combination $m_K + \mu_N - m_\Lambda \geq 320$ MeV, where μ_N is the nucleon chemical potential.

There are more applications of the RMF approach to the physics of baryonic systems with strange particles which could not be discussed here due to limited space. Hypernuclear magnetic moments and

currents [16], decays of hypernuclei [17] should be mentioned among others.

In the next section, we introduce the underlying RMF model. Application to hypernuclei and to multiply strange baryonic systems is presented in Section 3. In Section 4, we make use of the Σ^--atom data to extract information about the Σ-nucleus interaction and discuss implications for Σ hypernuclei. We apply the RMF model to the description of K^- (hyper)nuclei in Section 5. Conclusions are drawn in Section 6.

2 RMF formalism

We employed the relativistic mean field approach where the strong interactions among point-like hadrons are mediated by *effective* mesonic degrees of freedom. In the following calculations we started from the Lagrangian density:

$$\begin{aligned}\mathcal{L} &= \bar{B}\left[\mathrm{i}\gamma^\mu D_\mu - (M_B - g_{\sigma B}\sigma - g_{\sigma^* B}\sigma^*)\right] B \\ &+ (D_\mu K)^\dagger (D^\mu K) - (m_K^2 - g_{\sigma K} m_K \sigma - g_{\sigma^* K} m_K \sigma^*) K^\dagger K \\ &+ (\sigma, \sigma^*, \omega_\mu, \vec{\rho}_\mu, \phi_\mu, A_\mu \text{ free-field terms}) - U(\sigma) - V(\omega) + \mathcal{L}_{\mathrm{T}} \ ,\end{aligned} \tag{1}$$

which includes, besides the common isoscalar scalar (σ), isoscalar vector (ω), isovector vector (ρ), electromagnetic (A) fields and nonlinear selfcouplings $U(\sigma)$ and $V(\omega)$, also *hidden strangeness* isoscalar σ^* and ϕ fields which couple exclusively to strangeness degrees of freedom. Vector fields are coupled to baryons B (nucleons, hyperons) and K mesons via the covariant derivative:

$$D_\mu = \partial_\mu + \mathrm{i}\, g_{\omega\Phi}\, \omega_\mu + \mathrm{i}\, g_{\rho\Phi}\, \vec{I}\cdot\vec{\rho}_\mu + \mathrm{i}\, g_{\phi\Phi}\, \phi_\mu + \mathrm{i}\, e\, (I_3 + \tfrac{1}{2} Y_{\mathrm{H}}) A_\mu \ , \tag{2}$$

where $\Phi = B, K$, with $\vec{I}$ denoting the isospin operator, I_3 being its z component, and Y_{H} standing for hypercharge. Finally, the Lagrangian density $\mathcal{L}_{\mathrm{T}}$ (1) describes the ω-Y anomalous coupling,

$$\mathcal{L}_{\mathrm{T}} = \frac{f_{\omega Y}}{2M_Y}\, \bar{\Psi}_Y\, \sigma^{\mu\nu} \partial_\nu V_\mu \Psi_Y \ . \tag{3}$$

This term is essential in order to get a negligible spin-orbit splitting for the larger values of the Λ couplings required by constituent quark model [5]. It is to be noted that similar tensor coupling term for nucleons is omitted since the coupling constant $f_{\omega N}$ is small.

The system of coupled field equations for baryons ($N,\ \Lambda,\ \Sigma,\ \Xi$), antikaons and meson fields ($\sigma,\ \sigma^*,\ \omega,\ \rho,\ \phi,\ A$), which results from $\mathcal{L}$ (1) using standard techniques and approximations [1], is solved fully selfconsistently using an iterative procedure [5, 14]. This appeared crucial for the proper evaluation of the dynamical effects in the studied many-body hadronic systems.

$\bar{K}$ absorption modes were incorporated by adding an imaginary optical-model potential $\mathrm{Im}V_{\mathrm{opt}}$, with a strength determined by K^- atom fits and with energy dependence following decay phase-space. Suppression factors multiplying $\mathrm{Im}V_{\mathrm{opt}}$ were introduced to account for the reduction of the phase space available for $\bar{K}$ absorption from deeply bound states. Two absorption channels, $\bar{K}N \to \pi Y$ ($Y = \Sigma,\ \Lambda$) and $\bar{K}NN \to YN$, were considered [14].

To parametrize the nucleonic part of the Lagrangian density (1) we considered the standard RMF parameter sets NL-SH [18] and NL-TM1(2) [19] which have been successfully used in numerous calculations of various nuclear systems.

In the case of hyperons the coupling constants to the vector fields were fixed using SU(6) symmetry. For Λ hyperon this leads to

$$g_{\omega\Lambda} = \frac{2}{3} g_{\omega N},\ g_{\rho\Lambda} = 0,\ g_{\phi\Lambda} = \frac{-\sqrt{2}}{3} g_{\omega N}. \tag{4}$$

The coupling to the scalar σ field was then estimated by fitting to measured Λ-hypernuclear binding energies [20]. Finally, the uniquely identified hypernucleus ${}^{6}_{\Lambda\Lambda}$He served to fix the coupling to the σ^* field by fitting to the observed $\Delta B_{\Lambda\Lambda} \approx 1$ MeV [21]. For Ξ hyperons, SU(6) symmetry gives:

$$g_{\omega\Xi} = \frac{1}{3} g_{\omega N},\ g_{\rho\Xi} = -g_{\rho N},\ g_{\phi\Xi} = -2\frac{\sqrt{2}}{3} g_{\omega N}. \tag{5}$$

Since there are no experimental data for $\Xi(\Lambda)$-Ξ interactions, we set $g_{\phi\Xi} = g_{\sigma^*\Xi} = 0$ to avoid parameters that might lead to unphysical consequences and which, in addition, are expected to play a minor role. The coupling of the Ξ hyperon to the scalar σ field was constrained to yield an optical potential Re $V_{\Xi^-} = -14$ MeV in the center of ^{12}C [22]. The issue of Σ hyperon couplings is discussed in proper places in Sections 3 and 4.

For the antikaon couplings to the vector meson fields we adopted a purely F-type, vector SU(3) symmetry:

$$2g_{\omega K} = 2g_{\rho K} = \sqrt{2} g_{\phi K} = g_{\rho\pi} = 6.04, \tag{6}$$

where $g_{\rho\pi}$ is due to the $\rho \to 2\pi$ decay width [23]. The K^- coupling constants to the σ field, $g_{\sigma K}$, was varied in order to scan over a wide range of K^- binding energies. Furthermore, for use in multistrange configurations, the coupling constant to the σ^* field was taken from $f_0(980) \to K\bar{K}$ decay to be $g_{\sigma^* K} = 2.65$ [24]. The effect of the σ^* field was found generally to be minor. For a more comprehensive discussion of the choice of coupling constants, see Ref. [15].

We considered many-body systems consisting of the SU(3) octet N, Λ, Σ, and Ξ baryons that can be made particle-stable against strong interactions [8]. The energy release values Q for various conversion reactions of the type $B_1 B_2 \to B_3 B_4$ together with phenomenological guidance on hyperon–nucleus interactions suggest that only the conversions $\Xi^- p \to \Lambda\Lambda$ and $\Xi^0 n \to \Lambda\Lambda$ (for which $Q \simeq 20$ MeV) can be overcome by binding effects. It becomes possible then to form particle-stable multi-$\{N, \Lambda, \Xi\}$ configurations for which the conversion $\Xi N \to \Lambda\Lambda$ is Pauli blocked owing to the Λ orbitals being filled up to the Fermi level. For composite configurations with Σ hyperons the energy release in the $\Sigma N \to \Lambda N$ conversion is too high ($Q \gtrsim 75$ MeV) and, hence, it is unlikely for hypernuclear systems with Σ hyperons to be particle-stable.

3 Hypernuclei

3.1 Hypernuclear shell model

The RMF model introduced in Section 2 yields reasonable description of known hypernuclear characteristics – hyperon binding in nuclear matter, spin-orbit interaction, single particle spectra [5]. Here, we discuss the role of the tensor coupling (Eq.(9)) in evaluating the hypernuclear spin-orbit interaction. In Fig. 1, ${}^{17}_{Y}$O serves as an example of a quite different contribution of the tensor coupling term $\mathcal{L}_T$ to the spin-orbit splitting in a case of the three kinds of hyperons ($Y = \Lambda,\ \Sigma^0,\ \Xi^0$). It is to be stressed that for sake of comparison we adopted here the well depth of the Σ-nucleus and Ξ-nucleus potential of the same size as that for Λ, $U_\Sigma \approx U_\Xi \approx U_\Lambda$.

The results of Fig. 1 become apparent from the Schrödinger equivalent spin orbit potential:

$$\begin{aligned} V_{ls}^{Y}\ \vec{l}\cdot\vec{s} &= \frac{1}{2M_{\rm eff}^2}\left[\frac{1}{r}\left(g_{\omega Y}V_0' - g_{\sigma Y}\phi' + 2f_{\omega Y}\frac{M_{eff}}{M_Y}V_0'\right)\right]\vec{l}\cdot\vec{s}\,, \\ M_{\rm eff} &= M_Y - \frac{1}{2}\left(g_{\omega Y}V_0 - g_{\sigma Y}\phi\right)\ . \end{aligned}$$

For $f_{\omega Y} = 0$ the spin-orbit splitting for hyperons is reduced when compared to the nuclear case due to a larger mass $M_{\rm eff}$ in the denominator and due to smaller couplings to σ and ω mesons. The quark model values of $f_{\omega Y}$ for Λ, Σ and Ξ hyperons differ in their strengths and signs. Consequently, the tensor

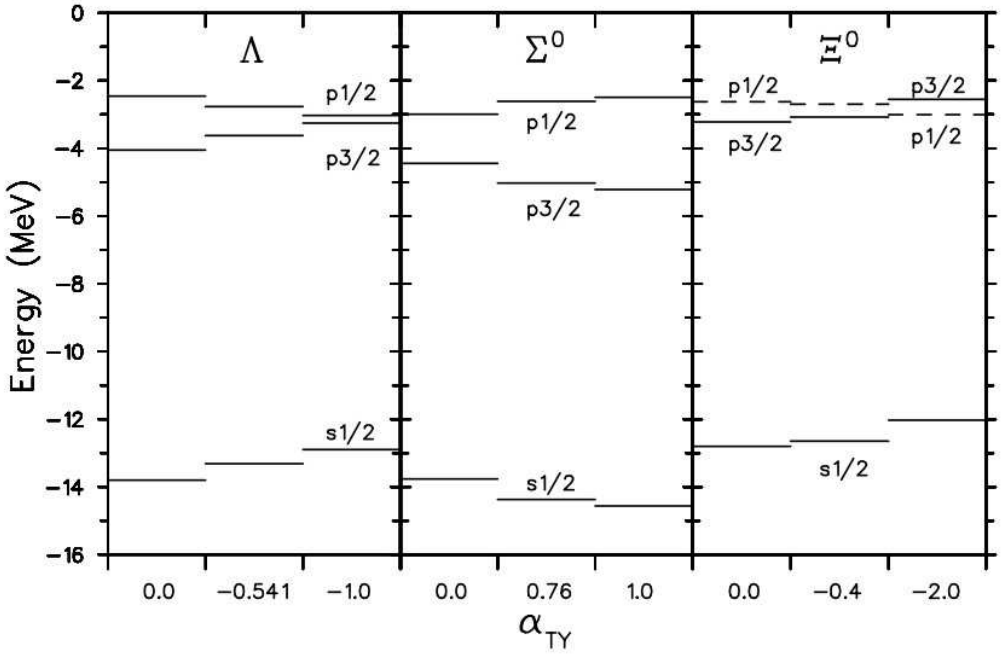

Fig. 1: Hyperon single-particle levels in ${}^{17}_{Y}$O as a function of $\alpha_{TY} = \frac{f_{\omega Y}}{g_{\omega Y}}$, for OBE model values (middle columns) and quark model values (right columns). See Ref. [5] for details.

coupling contribution is comparable in magnitude with the original $\sigma - \omega$ part and is negative (positive) for Λ (Σ). It is negative and even larger than $\sigma - \omega$ term for Ξ. The resulting spin-orbit interaction thus nearly vanishes for Λ, it is almost doubled for Σ, and changes sign for Ξ.

3.2 Multiply strange baryonic systems

The RMF model predicts a possibility of forming bound systems with an appreciable number of hyperons [6–8]. The dependence of the binding energies per particle, density distributions and rms radii of such systems on a number of hyperons n_Y, results from a delicate interplay between the effect of Pauli blocking (a hyperon is distinguishable from N), the weaker YN interaction compared to the NN one, and the conversion $\Lambda\Lambda \longrightarrow \Xi N$, which becomes energetically favorable due to the Pauli blocking of Λ's in some multi-Λ configurations [8]. The RMF calculations yield baryonic (N, Λ, Ξ) systems with densities $\rho \approx (2-3)\rho_0$, $|S|/A \approx 1$ and $|Z|/A \ll 1$. These baryonic objects are bound by $E_{\rm B}/A \approx 10-20$ MeV. Since it is much less than the $(\Lambda - N)$ mass difference (≈ 177 MeV), these objects will decay by weak interaction with lifetimes $\approx 10^{-10}$ s. An excellent review on the (N, Λ, Ξ) systems can be found in Ref. [8].

4 Σ^- atoms

Phenomenological analyses of level shifts and widths in Σ^- atoms by Batty et al. [25] suggested that the real part of the Σ-nucleus potential Re$V_{\rm opt}^{\Sigma}$ is attractive only at the nuclear surface, changing into a repulsive potential as density increases in the interior (for more details see Ref. [11]). The shallow attractive pocket of such potential does not provide sufficient binding to form Σ hypernuclei.

The RMF approach was applied directly to determining the Σ nucleus optical potential by fitting to Σ^- atom data in Ref. [9]. In this work, a real part of the Σ-nucleus potential was constructed out of the scalar (σ) and vector (ω, ρ) meson mean fields. A purely phenomenological imaginary part of

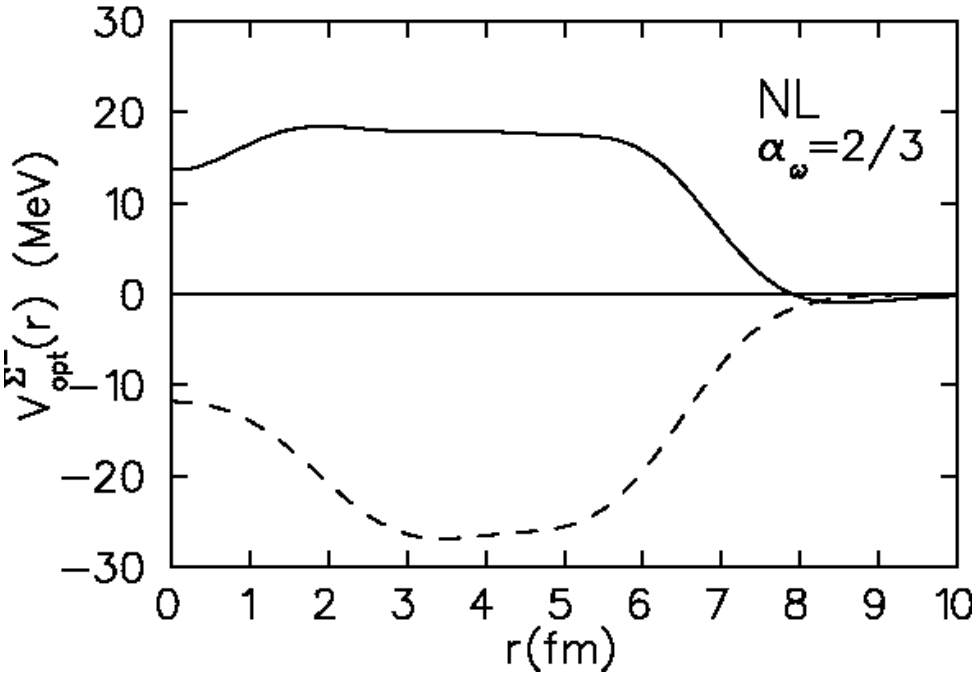

Fig. 2: Re$V^{\Sigma}_{\rm opt}$ (solid line) and Im$V^{\Sigma}_{\rm opt}$ (dashed line) as a function of r for the Σ^- optical potential in Pb.

the form Im$V^{\Sigma}_{\rm opt} = t\rho_p(r)$ was chosen in order to account for the conversion $\Sigma^- p \to \Lambda n$. While the proton density $\rho_p(r)$ was calculated within the RMF model, the parameter t was fitted to the atomic data. The other free parameters of the model were the scalar meson coupling ratio α_σ and isovector meson coupling ratio α_ρ ($\alpha_i = g_{i\Sigma}/g_{iN}$) . The values of the coupling ratio α_ω were adopted from constituent quark model ($\alpha_\omega = 2/3$) and QCD sum rules evaluations [26] (($\alpha_\omega = 1$).

The RMF approach is capable of very good quality fits to the Σ^-- atom data. It yields Re$V^{\Sigma}_{\rm opt}$ with a volume repulsion in the nuclear interior and a shallow attractive pocket at the surface in agreement with the density dependent phenomenological analyses [25]. For illustration, we show in Fig. 2 one of the Σ-nucleus potentials compatible with the data.

According to our calculations, the chances of establishing a meaningful Σ-hypernuclear spectroscopy are vanishingly small. Indeed, up to now, no Σ-hypernuclear bound state has been clearly established [27], except a $J^\pi = 0^+$, $I = 1/2$ ${}^{4}_{\Sigma}{\rm He}$ bound state [28], which is a too light system to be calculated within the RMF approach.

5 K^- (hyper)nuclei

The main objective of our recent calculations of K^--nuclear bound states was to establish correlations between various observables such as the K^- binding energy, width and macroscopic nuclear properties. By varying the K^- coupling constants $g_{\sigma K}$ we covered a wide range of binding energies and evaluated corresponding widths of K^- nuclear states.

Dynamically calculated widths Γ_{K^-} as function of the binding energy B_{K^-} are shown in Fig. 3 for $1s$ states in ${}^{12}_{K^-}$C, ${}^{16}_{K^-}$O, ${}^{40}_{K^-}$Ca and ${}^{208}_{K^-}$Pb. The dashed line shows the *static* nuclear-matter calculation for $\rho_0 = 0.16\ {\rm fm}^{-3}$, using the same kinematical phase-space suppression function. It is clearly seen that the dependence of the width of the K^- nuclear state on its binding energy follows closely the shape of the dotted line for the static nuclear-matter limit. This dependence is mainly due to the binding-energy dependence of the suppression factor which falls off rapidly until $B_{K^-} \sim 100$ MeV, where the dominant absorption mode $\bar{K}N \to \pi\Sigma$ gets switched off. In the range $B_{K^-} \sim 100 - 200$ MeV the width is

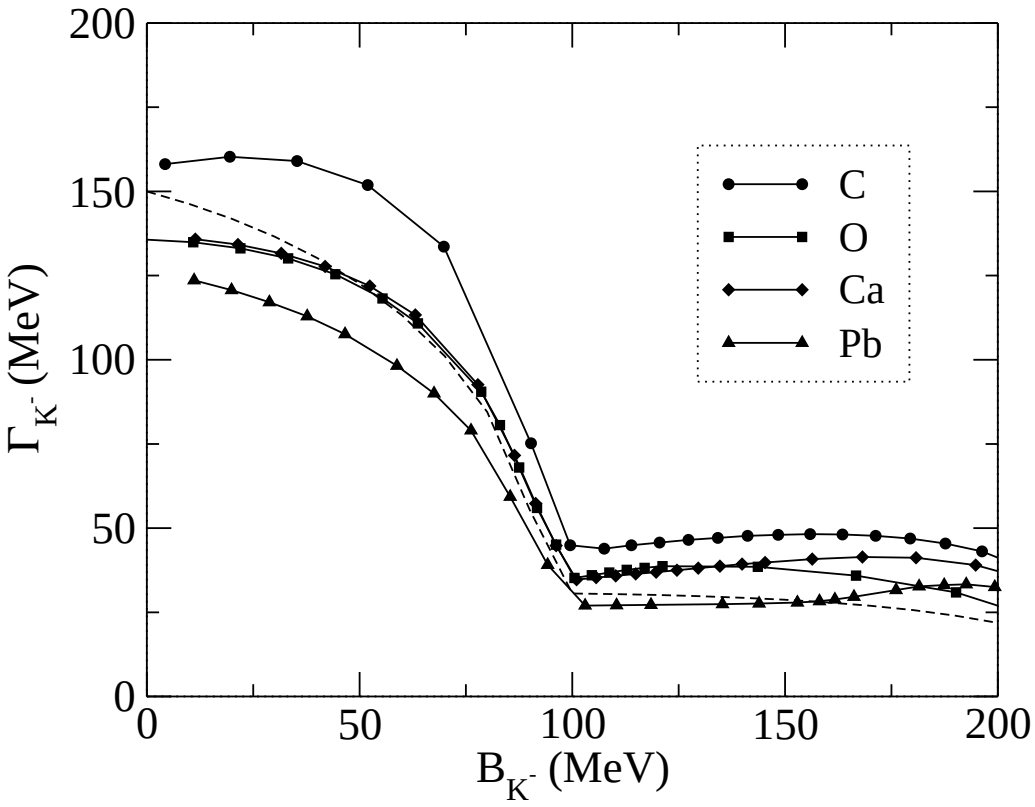

Fig. 3: Dynamically calculated widths of the 1s K^--nuclear state in ${}^{12}_{K^-}$C, ${}^{16}_{K^-}$O, ${}^{40}_{K^-}$Ca, and ${}^{208}_{K^-}$Pb as a function of the K^- binding energy. The dashed line indicates a static nuclear matter calculation.

dominated by the two-nucleon absorption mode. Here, the calculated widths for ^{12}C, ^{16}O and ^{40}Ca assume values $\Gamma_{K^-} = 45 \pm 5$ MeV, about a factor of two higher than what the static nuclear-matter calculation gives. This is due to the dynamical nature of the calculation whereby the nuclear density is enhanced.

Furthermore, in order to study effects of the nuclear polarization, we calculated rms radii, nuclear density distributions, and also single particle energies. Substantial polarization was found in light nuclei for deeply bound K^- nuclear states, with central nuclear densities about twice higher than for the corresponding nuclei without K^- [14].

In Ref. [15] we studied multi-K^- nuclei, observing that the calculated K^- separation energies as well as the nuclear densities saturate upon increasing the number of K^- mesons embedded in the nuclear medium. This saturation phenomenon, which is qualitatively independent of the applied RMF model, emerged for any boson-field composition containing the dominant vector ω-meson field which acts repulsively between K^- mesons. Since the calculated K^- separation energies did not exceed 200 MeV, for coupling-constant combinations designed to bind a single K^- meson in the range $B_{K^-} \sim 100 - 150$ MeV, it was argued that kaon condensation is unlikely to occur in strong-interaction self-bound hadronic matter. Here we demonstrate that these conclusions hold also when adding, within particle-stable multistrange configurations, large numbers of hyperons to nuclei across the periodic table. Figure 4 shows the calculated $1s$ K^- separation energy B_{K^-} in ${}^{40}\mathrm{Ca} + 20\Lambda + 2\Xi^0 + \kappa K^-$, ${}^{90}\mathrm{Zr} + 40\Lambda + 2\Xi^0 + 2\Xi^- + \kappa K^-$ and ${}^{208}\mathrm{Pb} + 106\Lambda + 8\Xi^0 + 18\Xi^- + \kappa K^-$ as a function of the number κ of K^- mesons.

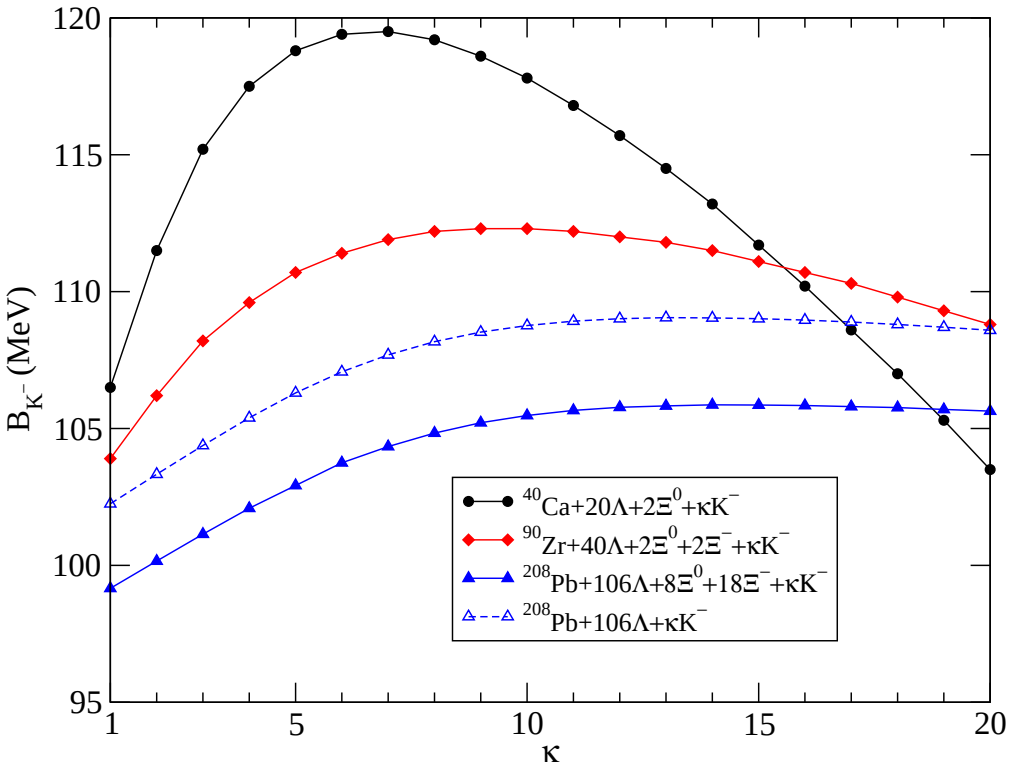

Fig. 4: The 1s K^- separation energy $B_{\bar{K}}$ in ^{16}O, ^{40}Ca, and ^{90}Zr with $\eta\Lambda + \mu\Xi + \kappa K^-$ as a function of the number κ of antikaons, for $B_{K^-} = 100$ MeV for $\kappa = 1$, $\eta = 0$.

6 Conclusions

This contribution aimed to demonstrate that the relativistic mean field approach provides a natural description of hyperon-nucleus and kaon-nucleus interactions:

With reasonable (quark model inspired) values of the meson-hyperon couplings it is possible to reproduce the hypernuclear data.

Extrapolation of the RMF theory from ordinary hypernuclei to multi-strange systems predicts rather weakly bound stable objects composed of N, Λ, and Ξ baryons, of arbitrarily large A, high strangeness content and small charge.

The Σ^--atom data are sufficient to significantly constrain the possible hyperon-nucleus couplings. The analysis yields potentials with a repulsive real part in the nuclear interior. Consequently, the chances of forming bound nuclear states of Σ (except perhaps the lightest systems) are very limited.

A lower limit $\Gamma_{K^-} = 45 \pm 5$ MeV was placed on the width expected for deeply bound K^- nuclear states in the range $B_{K^-} \sim 100 - 200$ MeV. The widths are mostly determined by phase-space suppression on top of the increase provided by the compressed nuclear density.

Multi-K^-–(hyper)nuclear calculations indicate that the binding energy per K^- meson saturates upon increasing the number of K^- mesons embedded in the nuclear medium. It is thus unlikely that kaon condensation occurs in strange hadronic matter.

Acknowledgments

Calculations and explorations which formed basis for this contribution were performed under fruitful and stimulating collaboration with E. Friedman, A. Gal, D. Gazda, and B.K. Jennings.
I would like to express my thanks to the organizers of the 12th International Conference on Nuclear Reaction Mechanisms in Varenna for their gracious hospitality.

References

[1] B.D. Serot, J.D. Walecka, Adv. Nucl. Phys. **16**, 1 (1986); Int. J. Mod. Phys. E **6**, 515 (1997).

[2] P. Bydžovský, A. Gal, J. Mareš (Eds.) , *Topics in Strangeness Nuclear Physics*, Lect. Notes Phys. 724 (Springer 2007); special issue of Nucl. Phys. A **804**, 1 (2008).

[3] N.K. Glendenning, *Compact Stars*, 2nd ed., (Springer 2000).

[4] W. Scheinast et al., Phys. Rev. Lett. **96**, 072301 (2006).

[5] J. Mareš, B.K. Jennings, Phys. Rev. C **49**, 2472 (1994).

[6] M. Rufa et al.: J. Phys. G **13**, 143 (1987).

[7] J. Mareš, J. Žofka, Z. Phys. A **333**, 209 (1989).

[8] J. Schaffner, C.B. Dover, A. Gal, C. Greiner, D.J. Millener, H. Stöcker, Ann. Phys. **235**, 35 (1994); J. Schaffner-Bielich, A. Gal, Phys. Rev. C **62**, 034311 (2000).

[9] J. Mareš, E. Friedman, A.Gal, B.K. Jennings, Nucl. Phys. A **594**, 311 (1995).

[10] C.J. Batty, E. Friedman, A. Gal, Phys. Rep. **287**, 385 (1997); E. Friedman, A. Gal, Phys. Rep. **452**, 89 (2007).

[11] E. Friedman, A. Gal, C.J. Batty, Phys. Lett. B **308** (1993) 6; E. Friedman, A. Gal, and J. Mareš, A. Cieplý, Phys. Rev. C **60**, 024314 (1999).

[12] A. Ramos, E. Oset, Nucl. Phys. A **671**, 481 (2000); A. Cieplý, E. Friedman, A. Gal, J. Mareš, Nucl. Phys. A **696**, 173 (2001).

[13] A. Gal, *Overview of $\bar{K}$-Nuclear Theory and Phenomenology*, arXiv: nucl-th/0703098.

[14] J. Mareš, E. Friedman, A. Gal, Nucl. Phys. A **770**, 84 (2006); D. Gazda, E. Friedman, A. Gal, J. Mareš, Phys. Rev. C **76**, 055204 (2007).

[15] D. Gazda, E. Friedman, A. Gal, J. Mareš, Phys. Rev. C **77**, 045206 (2008); D. Gazda, E. Friedman, A. Gal, J. Mareš, *Multi-$\bar{K}$ Hypernuclei*, arXiv: 0906.5344 [nucl-th].

[16] J. Cohen, J.V. Noble, Phys. Rev. **C46**, 801 (1992)

[17] A. Ramos, E. Van Meijgaard, C. Bennhold, B.K. Jennings, Nucl. Phys. **A544**, 703 (1992)

[18] M.M. Sharma, M.A. Nagarajan, P. Ring, Phys. Lett. B **312**, 377 (1993).

[19] Y. Sugahara, H. Toki, Nucl. Phys. A **579**, 557 (1994).

[20] O. Hashimoto, H. Tamura, Prog. Part. Nucl. Phys. **57**, 564 (2006).

[21] H. Takahashi *et al.*, Phys. Rev. Lett. **87**, 212502 (2001).

[22] P. Khaustov *et al.*, Phys. Rev. **61**, 054603 (2000).

[23] W. Weise, R. Härtle, Nucl. Phys. A **804**, 173 (2008).

[24] J. Schaffner, I.N. Mishustin, Phys. Rev. C **53**, 1416 (1996).

[25] C.J. Batty, E. Friedman, A. Gal, Phys. Lett. B **335**, 273 (1994).

[26] X. Jin and M. Nielsen, Phys. Rev. **C51**, 347 (1995).

[27] R. Sawafta, Nucl. Phys. A **585**, 103c (1995).

[28] R.S. Hayano et al., Phys. Lett. B **231**, 355 (1989).